New prompt fission neutron spectra measurements in the ^{238}U(n,f) reaction with a dedicated setup at LANSCE/WNR

Benoit Laurent[1,a], Paola Marini[1], Gilbert Bélier[1], Thomas Bonnet[1], Audrey Chatillon[1], Julien Taieb[1], David Etasse[2], Matthew Devlin[3], and Robert Haight[3]

[1] CEA, DAM, DIF, 91297 Arpajon, France
[2] LPC Caen, ENSICAEN, Université de Caen, CNRS/IN2P3, Caen, France
[3] P-27, Los Alamos National Laboratory, Los Alamos, NM 87544, USA

Abstract. A new prompt fission neutron spectra (PFNS) measurement in the ^{238}U(n,f) reaction was performed at LANSCE/WNR facility. Evaluated data show discrepancies on the low (below 1 MeV) and high (above 5 MeV) energy parts in the PFNS for different major and minor actinides. The goal is to improve these measurements in a wide range of incident energy.

The energy of the incoming neutron, inducing the fission, and the prompt neutron energies, are measured by time-of-flight method.

A dedicated fission chamber was developed, in order to improve alpha-fission discrimination, timing resolution, actinide mass, and to reduce the amount of neutron scattering. To detect prompt neutrons, the 54 Chi-Nu scintillator cells array were surrounding the fission chamber.

High statistics were recorded during this experiment, allowing a precise study of PFNS behavior as a function of incident neutron energy, from 1 MeV to 200 MeV. This experiment also showed that all the new tools developed to improve PFNS measurements are performing. Therefore, measurements of PFNS with others actinides such as ^{239}Pu are planned.

1. Introduction

The energy spectrum of prompt neutron emitted in neutron-induced fission (PFNS) is a quantity of high interest, for instance, for reactor physics, global security and fundamental understanding of the fission process. Unfortunately, the experimental data are rather scarce, specifically for the high energy neutron induced fission reactions. Recent publications [1,2] point out the needs on new experimental data to produce new PFNS evaluations with uncertainties for actinide nuclei in accordance with the Coordinated Research Project (CRP) "Evaluation of Prompt Fission Neutron Spectra of Actinides" established by the IAEA Nuclear Data Section in 2009 [3].

Our laboratory is involved, since 2000's, in PFNS measurements [4–6] but a special effort was done the last years to improve the accuracy and uncertainties [7,8]. New dedicated tools (fission chamber, electronics, data acquisition system) were developed and validated through new PFNS measurements. This article describe one of these experiments, using a ^{238}U fission chamber.

2. Experimental principle

The principle of PFNS measurements is to place a fission chamber, containing the studied actinide, in a neutron beam. This chamber allows to detect properly neutron induced fission events by separating alpha-decay events. An array of liquid scintillator cells surrounds the fission chamber, to detect outgoing neutrons, and gammas. Liquid scintillators, such as EJ-309, can however provide pulse-shape discrimination (PSD) to separate gamma rays from neutrons.

The PFNS are obtained with a time-of-flight measurement using the signals of fission chamber and scintillator. Moreover, measurements are made for a wide range of incident neutron energies. By using a pulsed beam, it is possible to measure fission by fission, the time-of-flight of the incoming neutron and therefore its energy. This technique is called the double time-of-flight method, as illustrated on Fig. 1.

The presented experiment was performed at the WNR facility of the Los Alamos National Science Center [9,10]. Incoming neutrons are produced by spallation of a pulsed proton beam accelerated up to 800 MeV on a tungsten target. Neutrons are then collimated to provide neutron beams to different flight courses. The setup was installed at approximatively 20 m from the source. Figure 2 is a picture of the fission chamber in the center of the 54 scintillator cells.

3. Experimental setup

3.1. Fission chamber

The fission chamber contains 72 deposits of ^{238}U (0.6 mg/cm^2 for a total mass of 360 mg). The alpha-fission discrimination is very good: fission detection efficiency is better than 95%. Moreover, dedicated pre-amplifiers were developed to match the detector characteristics. Hence, the timing resolution of the chamber is less

[a] e-mail: benoit.laurent@cea.fr

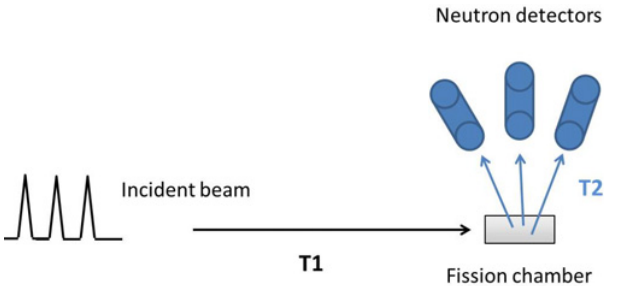

Figure 1. Double Time-of-flight technique: T1 stands for time-of-flight of incoming neutrons, T2 for outgoing neutrons.

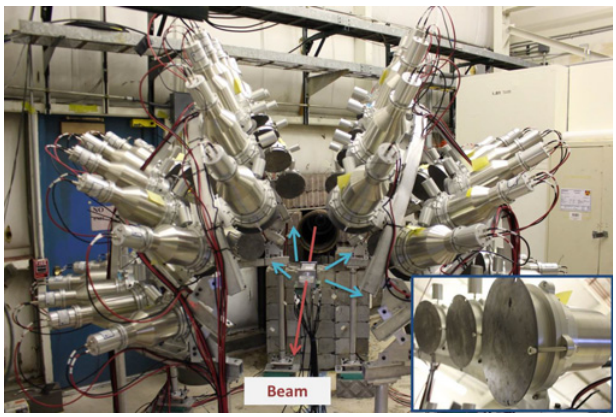

Figure 2. Picture of the fission chamber placed in the beam axis, surrounded by the 54 cells of Chi-Nu array. The incoming neutrons are schematized by the red arrow, the prompt fission neutrons by the blue arrows. The inset shows the lead shielding on the front face of each cell, as explained in Sect. 3.2.

than 0.8 ns FWHM, resulting in a timing resolution of the time-of-flight measurement of about 1.5 ns FWHM (these timing resolution was about 5 ns FWHM with our old setup). A total description of this chamber can be found in dedicated publication [11]. Chamber with identical housing, but containing only one deposit of ^{252}Cf (for further experiments, the ^{252}Cf will be equipped with a full stack of backing to mimic more precisely the actinide chamber) was used for neutron detection efficiency measurement purpose, assuming that the PFNS of ^{252}Cf(sf) is well known and recommended as a evaluated standard [12]. The very good alpha-fission discrimination of both chambers is illustrated on Fig. 3.

3.2. Neutron detection array

The neutron detector array is called Chi-Nu [13], and was built by the LANL. It consists of 54 EJ-309 liquid scintillator cells, coupled to photomultiplier tubes. The structure is composed of 6 lines of 9 cells, divided into two quarter of sphere, with a radius of about 1 m (flight path length of the fission neutrons).

EJ-309 is a typical liquid scintillator for neutron detection, which allows a neutron-gamma discrimination by pulse-shape analysis. Figure 4 shows a two-dimensional plot illustrating this discrimination, with two zones tagged as neutrons and gammas, and the resulting selected neutrons.

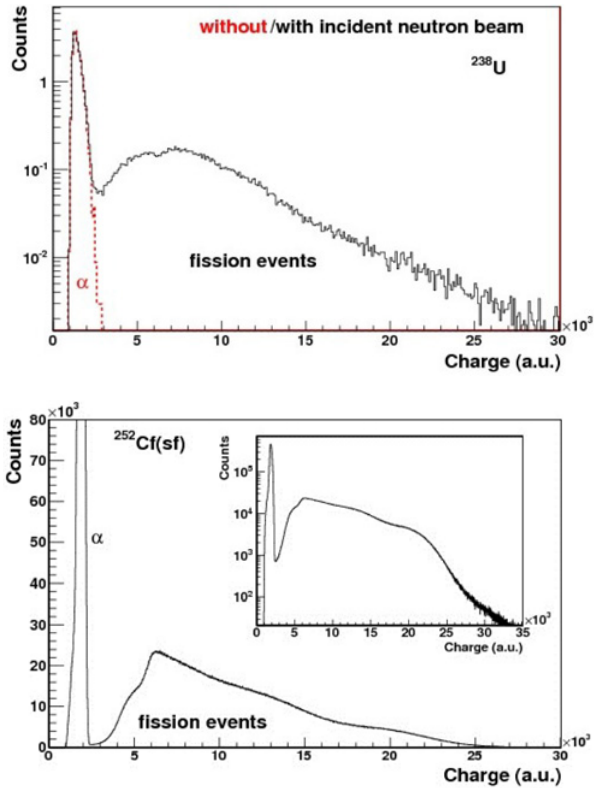

Figure 3. Pulse height spectra of the ^{238}U (upper part) and ^{252}Cf fission chamber (lower part), with a low fission event overlap.

By using lead shielding (see inset in Fig. 2), the amount of low energy gamma rays detected in the cells was reduced. Moreover, special efforts are made in the analysis method, to improve the neutron-gamma discrimination and the gamma rejection [14]. Combined to the digital acquisition system, allowing better performances, the threshold of the neutron detection was reduced by at least a factor two compared to previous experiments.

3.3. Data acquisition system

The data acquisition system used for these experiment is a digital system called FASTER (Fast Acquisition SysTem for nuclEar Research), currently being developed at LPC Caen [15]. Signals are digitized by a 500 MHz, 12-bits Analog-to-Digital low noise (1.1 lsb rms) Converter (ADC) and processed by real time numerical modules, implemented on FPGAs (Field Programmable Gate Array). The analog bandwidth of the sampling ADCs is limited at 100 MHz, thanks to a passive input low pass filter, in order to ensure a good zero time crossing determination on the Constant Fraction Discriminator (CFD) signal (using a 2nd order polynomial interpolation), and to optimize the signal over noise ratio. Finally, FASTER can provide a 7.8 ps-accuracy time data. The real time treatment is fast enough to allow a high counting rate (up to 700 000 events per second). Only relevant parameters (CFD timing, integrated charges, pulse height etc.) are stored. A graphical user interface and an online visualization program on the acquisition computer allow to setup and monitor all experiment parameters. Moreover, by absolute time stamping of each event, the reconstruction of coincidences off-line or a complex analysis is possible.

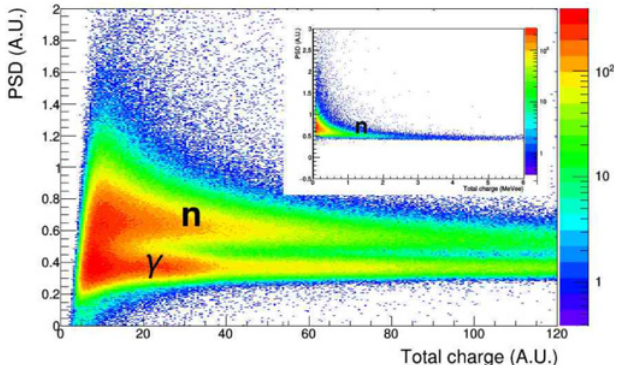

Figure 4. Pulse-shape discrimination as a function of total charge deposited in a cell by neutrons and gamma rays. The two zones are well identified, except at low charge where it is not possible to discriminate between both particles. This limit sets the threshold of neutron detection. The inset shows the selected neutrons after discrimination.

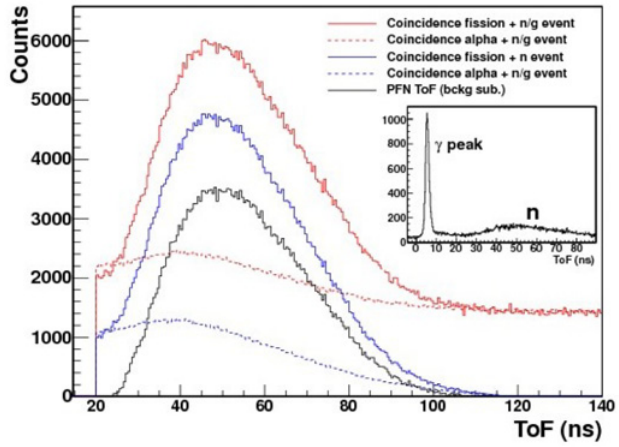

Figure 5. Time-of-flight spectrum for different type of coincidence event: fission trigger (solid line) or alpha trigger (dashed lines) with all events in scintillator cells (red) or only neutrons (blue). The black line is the time-of-flight result for the prompt fission neutrons (after background subtraction). The time-of-flight is cut below 20 ns to remove the prompt fission gamma peak and magnify the neutron bumps, but the inset shows the total ToF.

4. Data analysis

To extract prompt neutron time-of-flight, and therefore calculate their energy spectra, several analysis steps are needed. Alpha-fission discrimination in fission chamber has to be performed, as well as neutron-gamma discrimination in scintillator cells, in order to create time-of-flight with fission-neutron coincidence events. Part of the background due to incoming neutron scattering, or neutron coming from the environment (non-correlated to fission events) can be measured by trigging on alpha events in the fission chamber and analysing random coincidences in scintillator cells. This contribution can then be subtracted from the previous time-of-flight, as illustrated in Fig. 5.

Prompt fission neutrons can also scatter on the fission chamber, cells or environment materials before being detected, leading to a mis-measurement of their real time-of-flights, and then their energies. These neutrons are correlated to the fission events and can not be subtracted as in previous case.

However, since the neutron detection efficiency measurement with the ^{252}Cf is performed in the same conditions of environment, this contribution is corrected when the efficiency curve is applied to the raw data, assuming, in the first order, that the ^{252}Cf PFNS is similar enough to the ^{238}U PFNS. MCNPX [16] simulations, or dedicated efficency measurements, have to be performed to improve these corrections.

The neutron detection efficiency curve is obtained using ^{252}Cf data with the same analysis as for the ^{238}U (same thresholds, same discrimination cuts...). Then the measured energy spectra is divided by the Mannhart evaluated standard [12]. Figure 6 shows, as an example, the efficency curve for a selected one scintillator cell.

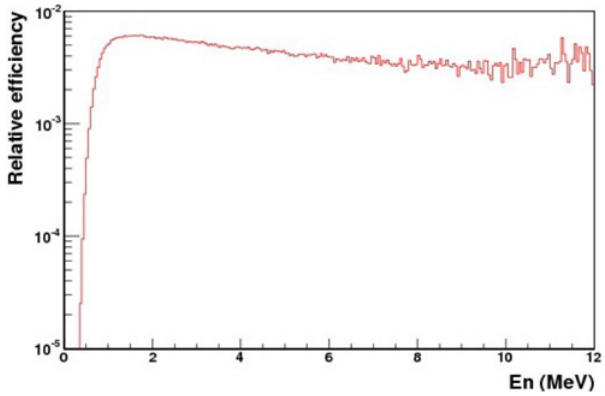

Figure 6. Neutron detection efficiency as a function of detected neutron energy for one of the Chi-Nu cells.

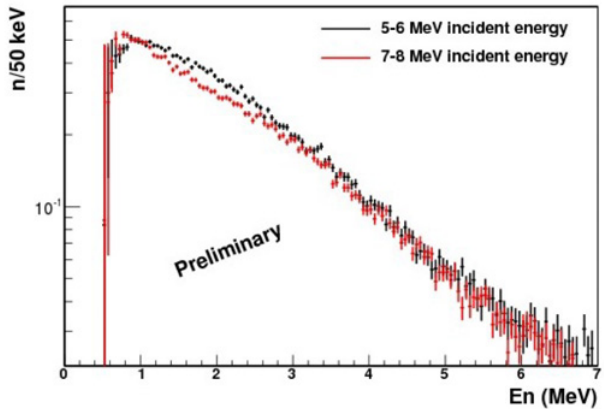

Figure 7. Preliminary energy spectra of prompt fission neutron in the ^{238}U(n,f) reaction, for two bins of incident energy (5–6 and 7–8 MeV), after efficiency corrections (curve in Fig. 6). This represents only a part of the whole statistics recorded during the experiment.

5. Preliminary experimental results

Once the analysis is performed, energy spectra can be obtained for each bin of incident energy, as showed as preliminary in Fig. 7. The neutron detection threshold achieved is about 500–600 keV.

With the LANSCE/WNR facility, the energy of the incoming neutron is in the 1-200 MeV range with a flux high enough for our purpose. Due to the beam pulsation,

the energy of the neutron inducing the fission can be measured by the time-of-flight technique (see Sect. 2), and the PFNS can be extracted for different bins in incident energy. It is then possible to follow the evolution of the spectra as a function of the incident energy, or to scan different zone, such as the opening of the x-th-chance fission.

The analysis is currently in progress and final and complete results will be published in forthcoming publications.

6. Incoming experiments

Others PFNS measurements are already accepted on different facilities. We plan to perform a ^{239}Pu(n,f) reaction measurement as LANSCE/WNR, with a dedicated fission chamber, similar to the one used for the ^{238}U, but more adapted to gloves box manipulation for deposits mounting, and with a geometry and electronics dedicated to very high alpha counting rate. We already demonstrated, by testing this new chamber with a 14 MBq ^{240}Pu deposits, that the fission detection efficiency is better than 90%. These high performances open the possibility of new measurements, which were not possible, or very difficult, till today.

We also proposed an experiment on the future GANIL/NFS facility, with a mono-kinetic incident neutron beam at 6.5 MeV. The goal is to measure the PFNS in the ^{238}U(n,f) reaction at the opening of the second chance fission. This measurement can bring constraint on compound emission (pre-fission neutrons) and on partial fission probabilities.

References

[1] R. Capote, Y.-J. Chen, F.-J. Hambsch, N.V. Kornilov, J.P. Lestone, O. Litaize, B. Morillon, D. Neudecker, S. Oberstedt, T. Ohsawa, N. Otuka, V.G. Pronyaev, A. Saxena, O. Serot, O.A. Shcherbakov, N.-C. Shu, D.L. Smith, P. Talou, A. Trkov, A.C. Tudora, R. Vogt, A.S. Vorobyev. Nuclear Data Sheets **131**, 1 (2016)

[2] D. Neudecker, T.N. Taddeucci, R.C. Haight, H.Y. Lee, M.C. White, M.E. Rising. Nuclear Data Sheets **131**, 289 (2016)

[3] R. Capote, V. Maslov, E. Bauge, T. Ohsawa, A. Vorobyev, M.B. Chadwick, S. Oberstedt. Summary Report, Consultants' Meeting on Prompt Fission Neutron Spectra of Major Actinides, IAEA-INDC, Vienna, INDC(NDS)-0541 (2009)

[4] T. Ethvignot, M. Devlin, R. Drosg, T. Granier, R.C. Haight, B. Morillon, R.O. Nelson, J.M. O'Donnell, and D. Rochman. Phys. Lett. B **575**, 221 (2003)

[5] J. Taieb, T. Granier, T. Ethvignot, M. Devlin, R.C. Haight, R.O. Nelson, J.M. O'Donnell, D. Rochman. Proceedings of the International Conference on Nuclear Data for Science and Technology, Nice, France, April 22–27, 2007, p. 429, 2007

[6] A. Chatillon, G. Bélier, T. Granier, B. Laurent, B. Morillon, J. Taieb, R.C. Haight, M. Devlin, R.O. Nelson, S. Noda, J.M. O'Donnell. Phys. Rev. C **89**, 014611 (2014)

[7] A. Sardet, C. Varignon, B. Laurent, T. Granier, A. Oberstedt. Nucl. Instr. and Meth. A **792**, 74–80 (2015)

[8] A. Sardet, PhD Thesis (2015)

[9] P.W. Lisowski, C.D. Bowman, G.J. Russell, S.A. Wender. Nucl. Sci. Eng. **106**, 208 (1990)

[10] P.W. Lisowski, K.F. Schoenberg. Nucl. Instr. and Meth. A **562**, 910–914 (2006)

[11] J. Taieb, B. Laurent, G. Bélier, A. Sardet, C. Varignon. Nucl. Instr. and Meth. A **833**, 1 (2016)

[12] W. Mannhart. Proceedings of the IAEA Advisory Group Mett. Properties of Neutron Sources, TECDOC-410, IAEA, Vienna, 158 (1987)

[13] R.C. Haight, H.Y. Lee, T.N. Taddeucci, J.M. O'Donnell, B.A. Perdue, N. Fotiades, M. Devlin, J.L. Ullmann, A. Laptev, T. Bredeweg, M. Jandel, R.O Nelson, S.A. Wender, C.-Y. Wu, E. Kwan, A. Chyzh, R. Henderson, J. Gostic. Proceedings of the 2nd International Workshop on Fast Neutron Detectors and Applications, Ein Gedi, Israel November 6-11, 2011, ed. A. Buffler, JINST 7, C03028 (2012)

[14] P. Marini. Private communication (2016)

[15] FASTER, `http://faster.in2p3.fr`, 2013

[16] D.B. Pelowitz, Ed. "MCNPX Users Manual Version 2.7.0" LA-CP-11-00438 (2011)